AIP | Applied Physics Letters

Coherent Raman scattering with three lasers

S. Chandra, A. Compaan, and E. Wiener-Avnear

Citation: Applied Physics Letters **33**, 867 (1978); doi: 10.1063/1.90194
View online: http://dx.doi.org/10.1063/1.90194
View Table of Contents: http://scitation.aip.org/content/aip/journal/apl/33/10?ver=pdfcov
Published by the AIP Publishing

Coherent Raman scattering with three lasers

S. Chandra, A. Compaan, and E. Wiener-Avnear[a)]

Department of Physics, Kansas State University, Manhattan, Kansas 66506
(Received 10 July 1978; accepted for publication 7 September 1978)

General conditions for four-wave mixing processes are investigated for the three-dimensional geometry. Unlike the standard two-frequency coherent Raman scattering, the use of three laser beams allows great flexibility in the phase-matching condition. Theoretically calculated plots are presented for dispersive and nondispersive media and are compared with experimental results in carbon disulphide and hydrogen gas, respectively.

PACS numbers: 42.65.−k, 42.10.Mg, 42.50.+q, 78.30.Cp

Four wave mixing processes such as coherent Stokes and coherent anti-Stokes Raman scattering (CSRS and CARS) require two or three intense coherent electromagnetic waves interacting in a nonlinear medium. Most CSRS and CARS experiments to date have been performed with only two incident laser frequencies, although, in principle, three input waves could be used with three distinct frequencies and three distinct wave-vector directions as well. Specialized examples of the use of three different laser frequencies[1,2] and of three wave vectors but only two frequencies[3,4] for CARS have been reported. The purpose of this letter is to point out the generalized energy and phase-matching conditions which apply when three incident laser frequencies are used. In addition, we present experimental results obtained in CS_2 and in H_2 which verify these relations and discuss some situations in which the flexibility inherent in the use of three laser frequencies will be advantageous.[5,6]

The interaction of three input laser waves mediated by a Raman or a two-photon absorption (TPA) resonance in a medium gives rise to the fourth (the signal) wave. The interaction is characterized by the absorption of two photons and emission of two other photons. The four waves will be identified by the subscripts $1, 2, p$, and q with $\omega_1 > \omega_2$ and $\omega_q > \omega_p$. For anti-Stokes shifts the input frequencies are labeled ω_1, ω_2, and ω_p and the signal occurs at $\omega_q = \omega_p + \omega_1 - \omega_2$. For Stokes shifts the input frequencies are labeled ω_1, ω_2, and ω_q and the signal occurs at $\omega_p = \omega_q - \omega_1 + \omega_2$. The energy and wave-vector conservation between the four waves can be expressed as

$$\omega_1 - \omega_2 = \omega_q - \omega_p \tag{1}$$

and

$$\mathbf{k}_1 - \mathbf{k}_2 = \mathbf{k}_q - \mathbf{k}_p. \tag{2}$$

A strong coherent Raman scattering (CARS or CSRS) will be observed when the frequency difference $(\omega_1 - \omega_2)$ is equal to a Raman resonance of the medium. Rearranging Eqs. (1) and (2) we obtain

$$\omega_1 + \omega_p = \omega_2 + \omega_q \tag{3}$$

and

$$\mathbf{k}_1 + \mathbf{k}_p = \mathbf{k}_2 + \mathbf{k}_q. \tag{4}$$

A strong signal will also be observed if the sum $(\omega_1 + \omega_p)$ is equal to a real two-photon absorption frequency of the medium. The four $\mathbf{k}_i$ vectors $(i = 1, 2, p, q)$ in Eqs. (2) and (4) need not all lie in the same plane.

Experimentally it is convenient to express the phase-matching conditions in terms of the angles between the various $\mathbf{k}_i$ vectors. From Eqs. (2) and (4) one can readily obtain

$$4k_q k_p \sin^2(\tfrac{1}{2}\delta) = 4k_1 k_2 \sin^2(\tfrac{1}{2}\beta) - (k_q - k_p + k_1 - k_2)\Delta k \tag{5}$$

and

$$4k_q k_2 \sin^2(\tfrac{1}{2}\gamma) = 4k_p k_1 \sin^2(\tfrac{1}{2}\alpha) + (k_q + k_p + k_1 + k_2)\Delta k, \tag{6}$$

where the angles α, β, γ, and δ are defined in the inset in Fig. 1 and Δk is the length mismatch between the magnitudes of the "outgoing" and "incoming" wave vectors:

$$\Delta k \equiv (k_q + k_2) - (k_1 + k_p). \tag{7}$$

One should note that for a nondispersive medium $\Delta k = 0$.

A third relation among the angles α, β, γ, and δ can be obtained for the general noncoplanar case. For clarity and convenience we will discuss the coplanar case since it exhibits most of the important features

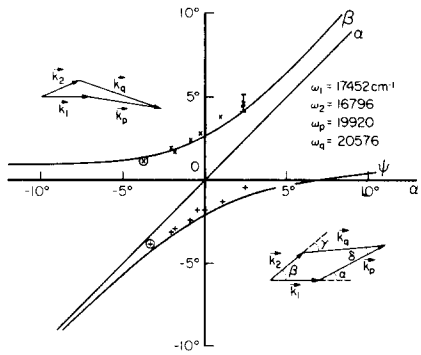

FIG 1. Phase matching for CARS in a dispersive medium. The input frequencies are ω_1, ω_2, and ω_p, where the difference $\omega_2 = 656\ \text{cm}^{-1}$ is equal to a Raman frequency of the medium, CS_2. The solid curves are calculated plots for the angles β, α, and ψ $(= \alpha - \delta)$ which the other three wave vectors make from $\mathbf{k}_1$. The plot of α versus α is included for easy visualization of the angular displacements of the various beams. The ×'s and +'s are experimentally measured values of β and ψ, respectively. The circled points correspond to simultaneous observation of two-laser CARS (signal at $2\omega_1 - \omega_2$) and a three laser CARS, $\omega_q = \omega_p + \omega_1 - \omega_2$. One should note that $\alpha > 0$ leads to a "box"-type geometry (lower right inset) and $\alpha < 0$ to a "bent" geometry (upper left inset).

[a)]Present address: Hughes Aircraft Company, 6155 El Camino Real, Carlsbad, 92008.

 0003-6951/78/3310-0867$00.50

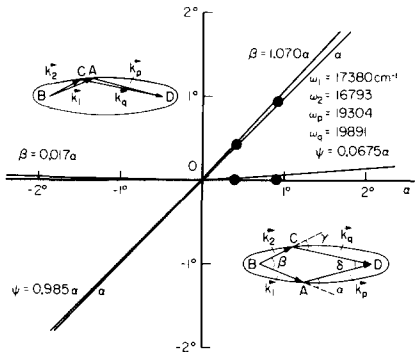

FIG. 2. CSRS in a nondispersive medium with input frequencies ω_1, ω_2, and ω_q, where the difference $\omega_1-\omega_2$ is equal to the 587-cm^{-1} rotational Raman frequency in hydrogen gas. One should note that for $\alpha>0$ the CSRS signal ω_p comes out angularly well separated from the probe ω_q, and one obtains a boxlike geometry. For a fixed value of $\mathbf{k}+\mathbf{k}_p$, the locus of points A and C lie on an ellipsoid of revolution with the foci separated by a distance equal to $\mathbf{k}_1+\mathbf{k}_p$.

inherent in the use of three independent laser beams. In the coplanar geometry the angles are further related by $(\alpha+\gamma)=(\beta+\delta)$. Taking the direction of $\mathbf{k}_1$ as reference, the angle ψ of $\mathbf{k}_q$ will be given by

$$\psi=\alpha-\delta=\beta-\gamma. \tag{8}$$

For further discussion on the features of the phase-matching condition we will examine various specialized geometries for dispersive and nondispersive[7] media. These categories are represented experimentally by the choice of carbon disulphide as an example of a dispersive medium and hydrogen gas as an example of a nondispersive medium. For the dispersive medium, viz., CS_2, the calculated curves based on Eqs. (5), (6), and (8) are shown in Fig. 1. In order to obtain the lengths of the wave vectors $k_i=n_i\omega_i/c$, the known values[8] of the refractive indices n_i were used for the frequencies shown in Fig. 1. In addition to the plots of β and ψ we have included a plot of α versus α, allowing one to visualize the relative angular displacements of various beams. These calculations were verified using an experimental arrangement similar to that used previously.[2] The principal modification was that the output beams of the double-frequency dye laser were separated out spatially and provided the frequencies ω_1 and ω_2. The third laser frequency ω_p beam was reflected to a 10-cm focusing lens using a dichroic mirror which transmitted ω_1 and ω_2. All three beams were parallel to one another when they reached the focusing lens. The angles between the focused beams were varied by varying the separation between beams before the lens. The experimental results shown are in good agreement with the calculated curves. The phase-matching geometries are either of the "bent" type (upper left inset in Fig. 1) corresponding to $\alpha<0$ or of the "box" type (lower right inset) corresponding to $\alpha>0$. Consider the following special cases: (i) The dividing line between the bent and box geometries is the triangle geometry corresponding to $\mathbf{k}_p\parallel\mathbf{k}_1$, i.e., $\alpha=0$. For this geometry one can readily show that

$$\sin^2(\tfrac{1}{2}\beta)=\frac{(k_q+k_1+k_p-k_2)\Delta k}{4k_2(k_1+k_p)}, \tag{9}$$

with similar expressions for $\sin^2(\frac{1}{2}\delta)$ and $\sin^2(\frac{1}{2}\gamma)$. For the particular case of Fig. 1 we see that for $\alpha=0$ we have $\beta=2.6°$ and $\psi=-\delta=-2.1°$. Physical values of the angles for this triangular geometry are possible only if $\Delta k\geq 0$. For a medium with linear dispersion, this requires $\omega_p\geq\omega_2$ if $\partial n/\partial\omega>0$ and $\omega_p\leq\omega_2$ if $\partial n/\partial\omega<0$. (ii) The standard two-frequency CARS corresponds to choosing $\mathbf{k}_p=\mathbf{k}_1$ and the signal is emitted at $\omega_q=2\omega_1-\omega_2$. One should note that it is possible to have the standard two-frequency CARS and a three-frequency CARS going at the same time. In such a case the angle β is fixed and the other angles can be selected to meet the phase-matching condition. The experimental observation of such simultaneous CARS is indicated by the circled points in Fig. 1. (iii) One may choose $\mathbf{k}_2\parallel\mathbf{k}_1$, i.e., $\beta=0$, which gives a triangular geometry once again. For this situation one obtains

$$\sin^2(\tfrac{1}{2}\alpha)=-\frac{(k_q+k_p+k_1-k_2)\Delta k}{4k_p(k_1-k_2)} \tag{10}$$

with similar expressions for $\sin^2(\frac{1}{2}\gamma)$ and $\sin^2(\frac{1}{2}\delta)$. This type of geometry was used by Laubereau *et al.*[3] (who further had $\omega_p=\omega_1$). Here, physical values of angles are possible only if $\Delta k\leq 0$. This means that for a positive dispersion medium $(\partial n/\partial\omega>0)$, one must have $\omega_p\leq\omega_2$ and for a negative dispersion medium $\omega_p\geq\omega_2$.

Next, let us discuss the nondispersive case. Figure 2 shows the calculated plots of the various angles for coherent Stokes-Raman scattering (CSRS) in hydrogen gas. The frequencies were chosen appropriate for the 587-cm^{-1} rotational Raman transition in hydrogen. The experimental points were obtained using the same experimental arrangement as for CS_2. Hydrogen gas was kept at a pressure of 15 atm in a 15-cm-long cell, and focusing of the beam was done using a 20-cm focal length lens. The cell windows limited the angles between the beams. For the boxlike geometry (lower right inset) there is a good separation between the angle ψ of the probe beam ω_q and the angle α of the CSRS signal ω_p. This should be contrasted with the bent geometry of the upper left inset where the signal will be emitted nearly collinearly with the probe beam. For the box geometry the angular separation of the signal ω_q from the laser ω_1 is seen to be directly related to their frequency difference; it is larger if $\omega_q-\omega_1$ is large.

For a nondispersive medium the magnitudes of the wave vectors are simply proportional to their respective frequencies. Then, from Eqs. (3) and (4) one can see that for a fixed $(\mathbf{k}_1+\mathbf{k}_p)$ the locus of points A and C (see the insets in Fig. 2) lies on an ellipsoid of revolution with foci at B and D and the separation BD equal to $(\mathbf{k}_1+\mathbf{k}_p)$. The major axis of the ellipsoid is equal to (k_1+k_p) and the minor axis equals $2(k_1k_p)^{1/2}\sin(\frac{1}{2}\alpha)$. Similarly, if one keeps $(\mathbf{k}_1-\mathbf{k}_2)$ fixed, the locus of points B and D from Eqs. (1) and (2) is seen to be a hyperboloid of revolution with major axis (k_1-k_2), minor axis $2(k_1k_2)^{1/2}\sin(\frac{1}{2}\beta)$, and the separation between foci AC equal to $(\mathbf{k}_1-\mathbf{k}_2)$.

Equations (5) and (6) together with $\Delta k=0$ are applicable for a general three-dimensional geometry. Several special geometries are experimentally convenient. (i) Choosing any one of the angles equal to zero is seen to make all the other angles zero and we have a com-

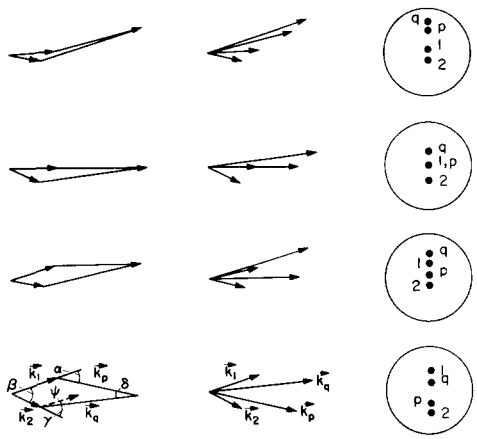

FIG. 3. The various geometries and relative ordering of the beams can all satisfy the phase-matching conditions for four-wave mixing. One obtains a box, triangle, or bent geometry, depending on whether the angle α is positive, zero, or negative, respectively.

pletely collinear geometry. This geometry although often used in CARS has the disadvantage of little spatial discrimination along the beam-propagation direction. (ii) The use of only two laser frequencies but three wave vectors for CARS corresponds to choosing $\omega_p = \omega_1$ but $\mathbf{k}_p \neq \mathbf{k}_1$ and $\alpha \neq 0$. This type of arrangement used by Eckbreth[4] in a coplanar geometry does allow for a spatial discrimination of the CARS signal ω_q and ω_1. (iii) Choosing $\omega_p = \omega_2$ leads to $\omega_q = \omega_1$, $\gamma = \alpha$, and $\delta = \beta$. The CARS signal will appear at the laser frequency ω_1 but will be emitted in the direction of ω_2.

The use of three laser frequencies allows a great deal of flexibility in the choice of angles (see Fig. 3) compared to the standard two-frequency CARS. The use of an additional laser does require having to superpose three laser beams in the medium and having to satisfy the more-complex phase-matching condition. It is often experimentally simpler to choose two of the beams collinear. With three incident lasers the coherent Raman signal was experimentally found to be linearly proportional to the intensities of each of the three lasers as expected. For the case of gases and also for small Raman shifts in dispersive media ($\Delta k \approx 0$) the use of three incident wave vectors offers the advantage of spatial discrimination of the signal. In addition, the use of three laser frequencies can be especially useful for the purpose of spectrally discriminating against laser light when Raman shifts are small. In CARS experiments, where dye lasers are used, fluorescence from the dye can be a problem for small Raman shifts. The use of a nondye laser (such as a frequency-doubled YAG : Nd^{3+} laser) for the third (probe) frequency will allow one to avoid any dye fluorescence and study CARS in a spectrally convenient regime.

In conclusion, the use of three lasers for coherent Raman scattering offers the capability for excellent spectral and spatial discrimination of the signal against noise via the great flexibility in the choice of various angles and frequencies.

[1]H. Lotem, R. T. Lynch, and N. Bloembergen, Phys. Rev. A **14**, 1748 (1976); R. T. Lynch, S. D. Kramer, H. Lotem, and N. Bloembergen, Opt. Comm. **16**, 372 (1976).

[2]A. Compaan, E. Wiener-Avnear, and S. Chandra, Phys. Rev. A **17**, 1083 (1978).

[3]A. Laubereau, G. Wockner, and W. Kaiser, Phys. Rev. A **13**, 2212 (1976).

[4]A. C. Eckbreth, Appl. Phys. Lett. **32**, 421 (1978).

[5]S. Chandra and A. Compaan, Bull. Am. Phys. Soc. **23**, 303 (1978).

[6]S. Chandra, E. Wiener-Avnear, and A. Compaan, J. Opt. Soc. Am. **68**, 633 (1978).

[7]Strictly speaking, there are no nondispersive materials. The term "nondispersive" is used in this paper to refer to situations where $(\Delta k/k)^{1/2}$ is less than the divergence of the incident laser beams after the focusing lens.

[8]*International Critical Tables* (McGraw-Hill, New York, 1929).